An Isogeometric Element Formulation for Linear Two-Dimensional Elasticity Based on the Airy Equation

S. Held*, W. Dornisch and N. Azizi

Chair of Structural Analysis and Dynamics
Brandenburg University of Technology Cottbus-Senftenberg
Cottbus, Germany
e-mail:{susanne.held, wolfgang.dornisch, nima.azizi}@b-tu.de

Key words: Airy equation, isogeometric analysis, two-dimensional elasticity, NURBS, element formulation

Abstract: *The aim of this work is to derive a formulation for linear two-dimensional elasticity using just one degree of freedom. This degree of freedom is used to directly discretize the Airy bipotential equation, which requires higher order basis functions. Isogeometric structural analysis is based on shape functions of the geometry description in Computer-Aided design software. These shape functions can easily fulfill the continuity requirement of the bipotential equation. Thus, an Airy element formulation can be obtained through isogeometric methods. In this contribution Non-Uniform Rational B-splines are used to discretize the domain and to solve the occurring differential equations. Numerical examples demonstrate the accuracy of the evolved formulation for a quadratic plate under different load situations.*

1 INTRODUCTION

In 2005 Hughes et. al [1] introduced isogeometric analysis (IGA). The basic idea of IGA is to use one common geometry model for design in Computer-Aided design (CAD) software and analysis with the finite element method (FEM) to overcome model conversions between design and analysis. Therefore the basis functions, commonly Non-Uniform Rational B-splines (NURBS) basis functions, from CAD models are also utilized as the basis for the FEM. Besides the exact description of the geometry, NURBS can also provide high inter-element continuity. That is why results of equal accuracy to standard FEM can be achieved using less elements. That points out the huge potential of IGA also for complex geometries. For further information on basics of NURBS, see [2, 3].

Compared to classical FEM, the numerical effort in IGA is slightly shifted from solving to assembly. Thus, currently a strong focus in IGA research is set on efficient integration rules, since the total number of integration points scales very well with the assembly costs. Initially, the use of full and reduced Gauss integration was proposed in [1, 4]. Currently, integration rules which are computed from moment fitting equations for specific problems have shown highly improved efficiency [5, 6, 7]. A very different idea to lower the computational effort for two-dimensional linear elasticity might be to further make use of the high continuity and choose to discretize not the standard weak form of equilibrium, but rather the well-known Airy equation, which is able to describe two-dimensional linear elasticity with only one unknown. This partial differential equation (PDE) combines the set of PDEs of the classical two-dimensional linear elasticity formulation approach. Instead of the two unknown displacements per control point of a standard two-dimensional elasticity formulation, with the discretized Airy formula only one degree of freedom per control point is obtained.

2 BASIC NURBS TERMINOLOGY FOR 2D ELASTICITY

The considered parameter space is subdivided into knot spans, denoted as elements. The knots are arranged as a non-decreasing array, the knot vector $\boldsymbol{\Xi} = \{\xi_1, \xi_2, ..., \xi_{n+p+1}\}$. Here, n

https://doi.org/10.4995/YIC2021.2021.12598

is the number of basis functions of polynomial order p needed for the B-spline construction. A B-spline curve $\mathbf{C}(\xi)$ is constructed through control points $\mathbf{B}_i$ using a set of polynomial basis functions $N_i^p(\xi)$ by

$$\mathbf{C}(\xi) = \sum_{i=1}^{n} N_i^p(\xi)\ \mathbf{B}_i\,. \tag{1}$$

The underlying p-th order basis functions $N_i^p(\xi)$ are defined as follows.

$$N_i^0(\xi) = \begin{cases} 1 & \text{if} \quad \xi_i \leq \xi \leq \xi_{i+1} \\ 0 & \text{else} \end{cases} \tag{2a}$$

$$p > 0 : N_i^p(\xi) = \frac{\xi - \xi_i}{\xi_{i+p} - \xi_i} N_i^{p-1}(\xi) + \frac{\xi_{i+p+1} - \xi}{\xi_{i+p+1} - \xi_{i+1}} N_{i+1}^{p-1}(\xi) \tag{2b}$$

The derivatives of the basis functions are always a combination of lower order basis functions. The k-th derivative of the i-th basis function can be generalized to

$$\frac{d^k}{d^k\xi} N_i^p(\xi) = \frac{p!}{(p-k)!} \sum_{j=0}^{k} \alpha_{k,j}\ N_{i+j}^{p-k}(\xi) \tag{3}$$

with $\alpha_{0,0} = 1,\ \alpha_{k,0} = \frac{\alpha_{k-1,0}}{\xi_{i+p-k+1} - \xi_i},\ \alpha_{k,k} = \frac{-\alpha_{k-1,k-1}}{\xi_{i+p+1} - \xi_{i+k}}\ \alpha_{k,j} = \frac{\alpha_{k-1,j} - \alpha_{k-1,j-1}}{\xi_{i+p+j-k+1} - \xi_{i+j}},\ \ j = 1, ..., k-1.$
Only a small step is necessary to transform the B-splines N_i^p to NURBS R_i^p. Every control point $\mathbf{B}_i = \left[\mathbf{X}_i^T, w_i\right]^T$ contains in addition to its coordinates $\mathbf{X}_i$ also a weight factor w_i. The B-spline basis has to be divided through the weighting function $W(\xi) = \sum_{i=1}^{n} N_i^p(\xi)\ w_i$.

$$R_i^p(\xi) = \frac{N_i^p(\xi)\ w_i}{W(\xi)}\,. \tag{4}$$

For the two-dimensional case the parameter space is spanned by a tensor product of knot vectors $\mathbf{\Xi}_1$ and $\mathbf{\Xi}_2$ in two directions which leads to the shape functions

$$N_I(\xi^1, \xi^2) = R_{ij}(\xi^1, \xi^2) = \frac{N_i^{p_1}(\xi^1) N_j^{p_2}(\xi^2) w_{ij}}{\sum_{\hat{i}=1}^{n_1} \sum_{\hat{j}=1}^{n_2} N_{\hat{i}}^{p_1}(\xi^1) N_{\hat{j}}^{p_2}(\xi^2) w_{\hat{i}\hat{j}}}. \tag{5}$$

Thus, the parametric coordinates of a surface point can be interpolated as

$$\mathbf{X}(\xi^1, \xi^2) = \sum_{I=1}^{n_{en}} N_I(\xi^1, \xi^2) \mathbf{X}_I\,, \tag{6}$$

where $n_{en} = (p_1 + 1)(p_2 + 1)$ is the number of control points per element. To obtain the element formulation using the solution method of Airy, derivatives up to the 4$^{\text{th}}$ order are required. For shape functions of two-dimensional spaces, partial derivatives have to be computed according to [2, pp. 136-138].

3 CONTINUUM MECHANICAL FORMULATION

In a two-dimensional space only displacements in two directions exist. Let $u_1 = u(x, y)$ be the displacement in x-direction and $u_2 = v(x, y)$ the displacement in y-direction. The underlying mechanics for a two-dimensional body in this space are described through the three

main conditions of kinematics, material and equilibrium. The kinematic relations state normal strains and shear strains as derivatives of the displacements

$$\varepsilon_x = \frac{\partial u}{\partial x}, \quad \varepsilon_y = \frac{\partial v}{\partial y}, \quad \gamma_{xy} = \frac{\partial v}{\partial x} + \frac{\partial u}{\partial y}. \tag{7}$$

The two mentioned displacements u and v cause normal stresses σ_{xx} and σ_{yy} in the directions x and y and shear stresses τ_{xy} or τ_{yx}. Although we presupposed only displacements in two directions and assume plane stress ($\sigma_{zz}, \tau_{xz}, \tau_{zx} = 0$), normal strains do also appear in the third direction. These correlations between stresses and strains are covered by the following material law for linear elasticity of a two-dimensional body

$$\varepsilon_x = \frac{1}{E}(\sigma_x - \nu\sigma_y), \quad \varepsilon_y = \frac{1}{E}(\sigma_y - \nu\sigma_x), \quad \varepsilon_z = -\frac{\nu}{E}(\sigma_x + \sigma_y) \tag{8a}$$

$$\gamma_{xy} = \frac{2(1+\nu)}{E}\tau_{xy}, \quad \gamma_{xz} = \gamma_{yz} = 0\,, \tag{8b}$$

where Young's modulus E and Poisson ratio ν are the material parameters. For applied loads f_x and f_y, equilibrium is given in x-direction and in y-direction by

$$\frac{\partial \sigma_{xx}}{\partial x} + \frac{\partial \tau_{xy}}{\partial y} + f_x = 0 \text{ and } \frac{\partial \sigma_{yy}}{\partial y} + \frac{\partial \tau_{yx}}{\partial x} + f_y = 0\,, \tag{9}$$

respectively. In order to ensure a steady and cohesive displacement, also the compatibility condition

$$\frac{\partial^2 \varepsilon_x}{\partial y^2} + \frac{\partial^2 \varepsilon_y}{\partial x^2} - \frac{\partial^2 \gamma_{xy}}{\partial x \partial y} = 0 \tag{10}$$

between the single strain components has to be fulfilled. Combining Eqs. (7) to (10), a biharmonic equation is received. For $f_x = f_y = 0$, we obtain the Airy-equation

$$\Delta\Delta F = 0\,, \tag{11}$$

where F denotes the Airy stress function, a measure without a further physical meaning. However, its second derivatives directly deliver the stresses

$$\sigma_{xx} = \frac{\partial^2 F}{\partial y^2}, \quad \sigma_{yy} = \frac{\partial^2 F}{\partial x^2}, \quad \tau_{xy} = -\frac{\partial^2 F}{\partial x \partial y}. \tag{12}$$

Taking into account the definition of the Laplace operator Δ, Eq. (11) is extended to

$$F_{,xxxx} + 2F_{,xxyy} + F_{,yyyy} = 0 \tag{13}$$

with $F_{,ijkl} = \frac{\partial}{\partial i}\frac{\partial}{\partial j}\frac{\partial}{\partial k}\frac{\partial}{\partial l}F$. This equation marks the starting point for developing the element formulation in the subsequent section.

4 NURBS-BASED ISOGEOMETRIC DISCRETIZATION

We suppose F to be a scalar field $F \in S$ with $S = \{F \in H^4(\Omega) | F = 0 \text{ on } \delta\Omega_D\}$ in the area of Ω. The corresponding test function is chosen as $\delta F \in S$. Eq. (13) is multiplied with the test function which yields three similar integrals of the type $\int_\Omega F_{,ijkl}\ \delta F \mathrm{da}$. Partial integration is applied two times and leads to:

$$\int_\Omega F_{,ijkl}\ \delta F\ \mathrm{da} = \int_\Omega (F_{,ijk}\ \delta F)_{,l}\ \mathrm{da} - \int_\Omega (F_{,ij}\ \delta F_{,l})_{,k}\ \mathrm{da} + \int_\Omega F_{,ij}\ \delta F_{,kl}\ \mathrm{da} \tag{14}$$

Using the divergence theorem for scalar values $\int_\Omega f_{,i}\ \mathrm{da} = \int_{\partial\Omega} f \cdot n_i\ \mathrm{ds}$, the integration space is reduced to the boundaries $\partial\Omega$ and the associated normal vector n_i is multiplied to the integral. For a rectangular domain these boundary integrals are treated separately for each boundary. At x-boundaries $n_x = 1,\ n_y = 0$ is valid and prescribed stresses $\sigma_{xx} = \overline{\sigma}_{xx}$ and $\tau_{xy} = \overline{\tau}_{xy}$ are considered. Equally at y-boundaries $n_x = 0,\ n_y = 1$ is valid and $\sigma_{yy} = \overline{\sigma}_{yy}$ and $\tau_{yx} = \overline{\tau}_{yx}$ are possible prescribed stresses. The divergence theorem is applied to Eq. (14) and the boundary terms are evaluated as mentioned. Thus, the final continuous element formulation is received:

$$\begin{aligned}
&\int_\Omega F_{,xxxx}\ \delta F\ \mathrm{da} + \int_\Omega F_{,yyyy}\ \delta F\ \mathrm{da} + \frac{1}{2}\ \int_\Omega F_{,xx}\ \delta F_{,yy}\ \mathrm{da} \\
&+\frac{1}{2}\ \int_\Omega F_{,yy}\ \delta F_{,xx}\ \mathrm{da} + \frac{1}{2}\ \int_\Omega F_{,xy}\ \delta F_{,yx}\ \mathrm{da} + \frac{1}{2}\ \int_\Omega F_{,yx}\ \delta F_{,xy}\ \mathrm{da} \\
&= \\
&+\frac{1}{2}\ \int_{\partial\Omega_x} \overline{\sigma}_{xx}\ \delta F_{,x}\ \mathrm{ds} + \frac{1}{2}\ \int_{\partial\Omega_y} \overline{\sigma}_{yy}\ \delta F_{,y}\ \mathrm{ds} - \frac{1}{2}\ \int_{\partial\Omega_x} \overline{\tau}_{xy}\ \delta F_{,y}\ \mathrm{ds} \\
&-\frac{1}{2}\ \int_{\partial\Omega_y} \overline{\tau}_{yx}\ \delta F_{,x}\ \mathrm{ds} + \frac{1}{2}\ \int_{\partial\Omega_x} \overline{\tau}_{xy,y}\ \delta F\ \mathrm{ds} + \frac{1}{2}\ \int_{\partial\Omega_y} \overline{\tau}_{yx,x}\ \delta F\ \mathrm{ds}
\end{aligned} \tag{15}$$

4.1 Interpolation of geometry, unknowns and test functions

The geometry is interpolated as in Eq. (6). To solve the continuum formulation given in Eq. (15), next to geometry also all other expressions in the function space are discretized as an interpolation over all control points. The approximations F^h and δF^h of the unknown Airy function and the corresponding test function are interpolated as follows:

$$F^h = \sum_{I=1}^{n_{np}} N_I\ F_I, \quad \delta F^h = \sum_{J=1}^{n_{np}} N_J\ \delta F_J \tag{16}$$

Eq. (15) requires up to the fourth derivative of the Airy function and up to the second derivative of the test function. They are easily derived from Eq. (16) since F_I and ∂F_I are discrete values. This leads to the following general derivatives with respect to global coordinates (x, y):

$$F^h_{,i} = \sum_{I=1}^{n_{np}} N_{I,i}\ F_I, \quad F^h_{,ij} = \sum_{I=1}^{n_{np}} N_{I,ij}\ F_I, \quad F^h_{,ijk} = \sum_{I=1}^{n_{np}} N_{I,ijk}\ F_I, \quad F^h_{,ijkl} = \sum_{I=1}^{n_{np}} N_{I,ijkl}\ F_I \tag{17}$$

$$\delta F^h_{,i} = \sum_{J=1}^{n_{np}} N_{J,i}\ \delta F_J, \quad \delta F^h_{,ij} = \sum_{J=1}^{n_{np}} N_{J,ij}\ \delta F_J \tag{18}$$

Later on, integration will be performed as Gaussian quadrature on a bi-unit parent element using classical change of variables formulation taking into account the Jacobian determinant. Computation rules of NURBS shape functions and their derivatives in Sec. 2 are based on the (ξ^1, ξ^2) coordinate system as needed in the integration process. Thus a transformation rule for the first, second and fourth derivatives of shape functions appearing on the left side in Eq. (15) is required between (x, y) and (ξ^1, ξ^2) coordinate system. As shown in [3] it is useful to apply the chain rule

$$\frac{\partial N}{\partial x_i} = \frac{\partial N}{\partial \xi^\alpha}\frac{\partial \xi^\alpha}{\partial x_i}\,. \tag{19a}$$

The gradient of this mapping $\frac{\partial x_i}{\partial \xi^\alpha}$ is computed as part of the Jacobian. To keep it simple yet exact for our purposes which only include rectangular domains, higher order derivatives are calculated as follows:

$$\frac{\partial^2 N}{\partial x_i\ \partial x_j} = \frac{\partial^2 N}{\partial \xi^\alpha\ \partial \xi^\beta}\frac{\partial \xi^\alpha}{\partial x_i}\frac{\partial \xi^\beta}{\partial x_j} \tag{19b}$$

$$\frac{\partial^4 N}{\partial x_i\,\partial x_j\,\partial x_k\,\partial x_l} = \frac{\partial^4 N}{\partial \xi^\alpha\,\partial \xi^\beta\,\partial \xi^\gamma\,\partial \xi^\delta}\frac{\partial \xi^\alpha}{\partial x_i}\frac{\partial \xi^\beta}{\partial x_j}\frac{\partial \xi^\gamma}{\partial x_k}\frac{\partial \xi^\delta}{\partial x_l} \tag{19c}$$

4.2 Formulation of the condition matrix and final system of equations

Implementing the discretizations and moving the discrete values of Airy and test function out of the integrals in Eq. (15) leads to

$$\begin{aligned}
&\sum_I^{n_{np}}\sum_J^{n_{np}}\Bigg[\Bigg(\int_\Omega N_{I,xxxx}\;N_J\;\mathrm{da}+\int_\Omega N_{I,yyyy}\;N_J\;\mathrm{da}+\frac{1}{2}\int_\Omega N_{I,xx}\;N_{J,yy}\;\mathrm{da}\\
&+\frac{1}{2}\int_\Omega N_{I,yy}\;N_{J,xx}\;\mathrm{da}+\frac{1}{2}\int_\Omega N_{I,xy}\;N_{J,yx}\;\mathrm{da}+\frac{1}{2}\int_\Omega N_{I,yx}\;N_{J,xx}\;\mathrm{da}\Bigg)\;F_I\;\delta F_J\Bigg]\\
&=\sum_J^{n_{np}}\Bigg[\Bigg(\frac{1}{2}\int_{\partial\Omega_x}\overline{\sigma}_{xx}\;N_{J,x}\;\mathrm{ds}+\frac{1}{2}\int_{\partial\Omega_y}\overline{\sigma}_{yy}\;N_{J,y}\;\mathrm{ds}-\frac{1}{2}\int_{\partial\Omega_x}\overline{\tau}_{xy}\;N_{J,y}\;\mathrm{ds}-\frac{1}{2}\int_{\partial\Omega_y}\overline{\tau}_{yx}\;N_{J,x}\;\mathrm{ds}\\
&\qquad+\int_{\partial\Omega_x}\overline{\tau}_{xy,y}\;N_J\;\mathrm{ds}+\int_{\partial\Omega_y}\overline{\tau}_{yx,x}\;N_J\;\mathrm{ds}\Bigg)\;\delta F_J\Bigg].
\end{aligned} \tag{20}$$

The left side of Eq. (20) represents the system "stiffness" $\mathbf{B}$ and as in most cases the right side includes the loading. To avoid mistakes in the usage of F as Airy stress function, the loads are marked as $\mathbf{L}$. A loop over all n_{el} elements will sum up the individual parts B^e_{IJ} of the condition matrix and load components L^e_J. This changes Eq. (20) to

$$\bigcup_{e=1}^{n_{el}}\sum_{I=1}^{n_{nen}}\sum_{J=1}^{n_{nen}} B^e_{IJ}\;F_I\;\delta F_J=\bigcup_{e=1}^{n_{el}}\sum_{J=1}^{n_{nen}} L^e_J\;\delta F_J. \tag{21}$$

For an efficient computation of results, Eq. (21) has to be brought into a system of equations. Therefore, the element condition matrix and the load vector can be arranged as

$$\mathbf{B}^e=\begin{bmatrix} B^e_{11} & \dots & B^e_{1n_{en}}\\ \vdots & \ddots & \vdots\\ B^e_{n_{en}1} & \dots & B^e_{n_{en}n_{en}}\end{bmatrix},\quad \mathbf{L}^e=\begin{bmatrix} L^e_1\\ \vdots\\ L^e_{n_{en}}\end{bmatrix}. \tag{22}$$

To solve the global system of equations all element matrices and load vectors have to be mapped to a global condition matrix $\mathbf{B}$ and the global load vector $\mathbf{L}$, respectively. In addition to that, the discrete solution values are arranged in a vector $\hat{\mathbf{F}}=\left[F_1,\dots,F_{n_{np}}\right]^T$, where n_{np} is the number of global degrees of freedom. After converting Eq. (21) such that the test function is dropped, the final system of equations

$$\mathbf{B}\;\hat{\mathbf{F}}=\mathbf{L} \tag{23}$$

can be solved for $\hat{\mathbf{F}}$ with standard routines.

4.3 Treatment of boundary conditions

The right side of the derived element formulation in Eq. (20) involves already prescribed stresses. These stresses are handed in the process of computation as specified neumann boundary conditions. They can be treated easily as they are well known. But it is much more of interest how to prescribe dirichlet boundary conditions. They do not directly enter the formulatiom, but are necessary to receive full rank for the condition matrix. Without them a too wide

solution space of possible stress functions, leading all to the correct stress state, is spanned. As in all FEM formulations dirichlet boundary conditions are imposed for the unknown degrees of freedom. For the presented element formulation this means some values for F have to be prescribed without knowing the correct mechanical interpretation. Since within this work only stress boundary conditions are treated, any dirichlet conditions can be set which yields a stable computation. It is important that there are enough, yet not too many independent prescribed values in order to obtain a stable solution. As in standard two-dimensional plane stress FEM, it is required to set at least three nodal dirichlet conditions in order to prevent the three rigid body modes. More boundary conditions should not be set in order to not overconstrain the solution. As displacement boundary conditions are usually the dirichlet conditions in standard FEM formulations, it has to be stated out that displacements are not concerned and this procedure does only guarantee accuracy for the stress state.

5 NUMERICAL EXAMPLES

For the following numerical examples, the derived element formulation was embedded in a matlab working routine for IGA. The expressions $\overline{\tau}_{xy,y}$ and $\overline{\tau}_{yx,x}$ are neglected since the examples include only constant or even no shear. The formulation is tested on a quadratic plate with the dimensions 2×2. As dirichlet condition, F was fixed in both bottom corners and the upper left corner of the plate.

5.1 Quadratic plate under linearly varying uniaxial tension

A linearly varying tension along the vertical boundaries is applied in x-direction. At the upper boundary a positive and at the lower boundary a negative stress of 10 is prescribed. The exact solution for σ_{xx} is constant in x-direction and varies linearly in y-direction as the

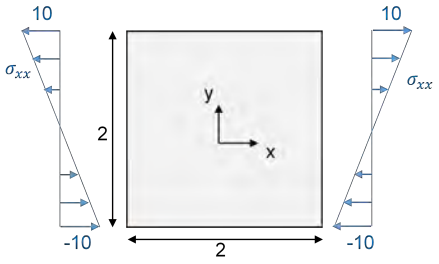

Figure 1: System sketch for quadratic plate under uniaxial tension

prescribed stresses. σ_{yy} and τ_{xy} are equal to zero. The stress results using the developed element formulation are provided in Figs. 2 to 4.

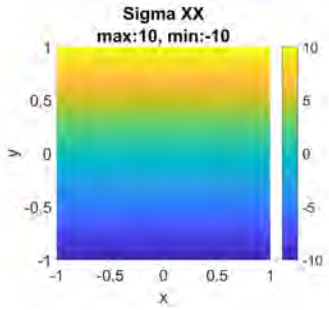

Figure 2: Stress σ_{xx} for quadratic plate under uniaxial tension

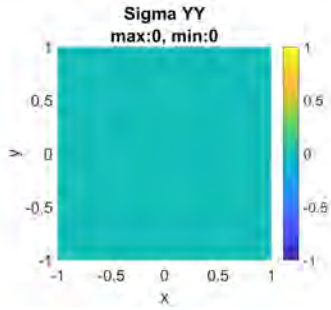

Figure 3: Stress σ_{yy} for quadratic plate under uniaxial tension

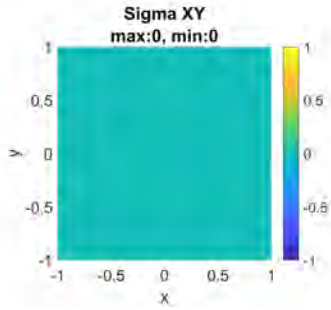

Figure 4: Stress τ_{xy} for quadratic plate under uniaxial tension

The mentioned exact analytic stress distribution can be found in all three stress plots. The values of τ_{xy} and σ_{yy} are actually numerical zero, only small computing errors in the range of the employed numerical precision appear. All discretizations yield the exact solution. This was also tested by the L_2-error norm. A negligible error in the range of 10^{-14} appeared for all refinement steps. To fulfill the condition of a full rank matrix three nodal dirichlet conditions have to be set.

5.2 Quadratic plate under pure shear

For the example of pure shear only shear stresses were prescribed at every boundary. As it is shown in the system sketch in Fig. 5, the unit square is constantly loaded with shear stresses of 10. The exact solution for τ_{xy} is constantly 10 over the whole plate while σ_{xx} and σ_{yy} are

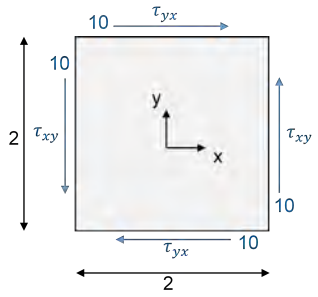

Figure 5: System sketch for quadratic plate under pure shear

equal to zero. For all three stresses the results are shown in Figs. 6 to 8. In the case of pure

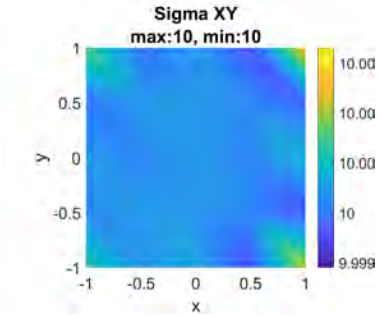

Figure 6: Stress τ_{xy} for quadratic plate under pure shear

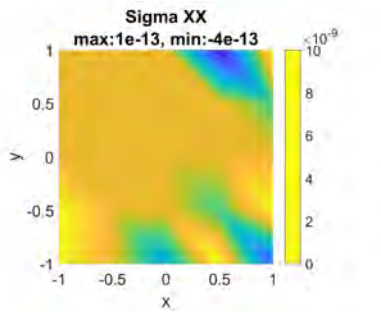

Figure 7: Stress σ_{xx} for quadratic plate under pure shear

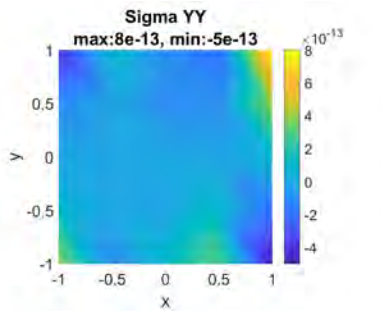

Figure 8: Stress σ_{yy} for quadratic plate under pure shear

shear the L_2-error norm is in the range of 10^{-13}, see Figs. 6 to 8. Under pure shear, as shown before under uniaxial tension, the exact solution can be obtained using just one element.

5.3 Quadratic plate under complex loads

A rectangular plate with the dimensions $-b \leq x \leq b$ and $-a \leq y \leq a$ is subjected to a complex load, which is derived from a chosen load function. This procedure is analogous to the method of manufactured solutions [8]. Here, a solution F is chosen, which is a simplified

version of the Fourier solution

$$\begin{aligned} F = &\sum_{n=1}^{\infty} \cos\beta_n x \left[B_n \cosh\beta_n y + C_n \beta_n y \sinh\beta_n y\right] \\ &+ \sum_{m=1}^{\infty} \cos\alpha_m y \left[D_m \cosh\alpha_m x + E_m \alpha_m x \sinh\alpha_m x\right] \end{aligned} \tag{24}$$

for uniaxial loading in y-direction with arbitrary shape but opposite sign on top and bottom, which is provided, e.g., in [9, pp. 175-178]. Since the complete Fourier solution is hard to compute with high precision, we simply use the solution with one Fourier term only. The stresses at the boundary are computed from this truncated solution and are applied as loading at the boundaries. Thus, we have loading functions at the boundary and at the same time we know the exact stress solution in every point within the domain. Since the occurring trigonometric functions and hyperbolic functions cannot be exactly described by NURBS basis functions, it is possible to study the convergence rates of the formulation.

The Airy function for this example is

$$\begin{aligned} F = &\cos\beta x \left[B \cosh\beta y + C\beta y \sinh\beta y\right] \\ &+ \cos\alpha y \left[D \cosh\alpha x + E\alpha x \sinh\alpha x\right] , \end{aligned} \tag{25}$$

where the constants are chosen in a way that the shear stresses τ_{xy} are zero along all boundaries. This yields $\alpha = \pi/a$, $\beta = \pi/b$,

$$D = -E(1 + \alpha b \coth\frac{\pi b}{a}) \qquad \text{and} \qquad B = -C(1 + \beta a \coth\frac{\pi a}{b}) . \tag{26}$$

Introducing Eq. (26) into Eq. (25) and using the required derivatives, the exact stresses are given by

$$\begin{aligned} \sigma_{xx} = &\beta^2 C \cos\beta x \left[\cosh\beta y + \beta y \sinh\beta y - \beta a \coth\frac{\pi a}{b} \cosh\beta y\right] \\ &- \alpha^2 E \cos\alpha y \left[\alpha x \sinh\alpha x - \cosh\alpha x - \alpha b \coth\frac{\pi b}{a} \cosh\alpha x\right] \\ \sigma_{yy} = &-\beta^2 C \cos\beta x \left[-\cosh\beta y + \beta y \sinh\beta y - \beta a \coth\frac{\pi a}{b} \cosh\beta y\right] \\ &+ \alpha^2 E \cos\alpha y \left[\alpha x \sinh\alpha x + \cosh\alpha x - \alpha b \coth\frac{\pi b}{a} \cosh\alpha x\right] \\ \tau_{xy} = &\beta^2 C \sin\beta x \left[\beta y \cosh\beta y - \beta a \coth\frac{\pi a}{b} \sinh\beta y\right] \\ &+ \alpha^2 E \sin\alpha y \left[\alpha x \cosh\alpha x - \alpha b \coth\frac{\pi b}{a} \sinh\alpha x\right] \end{aligned} \tag{27}$$

and can directly be used for the validation of the presented element formulation.

For the chosen domain it holds $a = 1$ and $b = 1$. The constants C and E, which basically govern the size of the load at the boundaries, are chosen to be $C = 10$ and $E = 1$. The resulting (Neumann) boundary condition are

$$\begin{aligned} \bar{\sigma}_{xx} = &\mp 10\beta^2 \left[\cosh\beta y + \beta y \sinh\beta y - \pi \coth\pi \cosh\beta y\right] \\ &\pm \alpha^2 \cos\alpha y \left[\pi \sinh\pi - \cosh\pi - \pi \coth\pi \cosh\pi\right] \end{aligned} \tag{28}$$

at $x = \pm b$ and

$$\begin{aligned} \bar{\sigma}_{yy} = &\pm 10\beta^2 \cos\beta x \left[-\cosh\pi + \pi \sinh\pi - \pi \coth\pi \cosh\pi\right] \\ &\pm \alpha^2 \left[\alpha x \sinh\alpha x + \cosh\alpha x - \pi \coth\pi \cosh\alpha x\right] \end{aligned} \tag{29}$$

at $y = \pm a$. At all boundaries $\bar{\tau}_{xy} = 0$ holds.

The following results in Figs. 9 to 11 are obtained from NURBS of order $p = 8$ using 50×50 elements within the patch. The error of the plotted stresses is in the range of 10^{-6}.

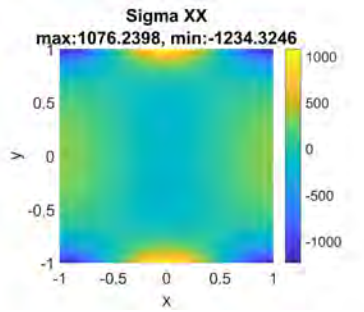

Figure 9: Stress σ_{xx} for quadratic plate under complex load

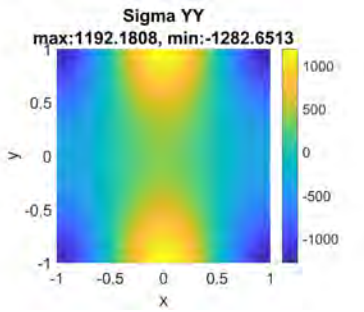

Figure 10: Stress σ_{yy} for quadratic plate under complex load

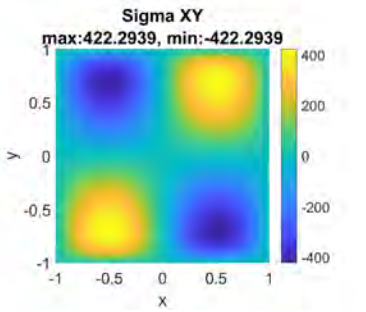

Figure 11: Stress τ_{xy} for quadratic plate under complex load

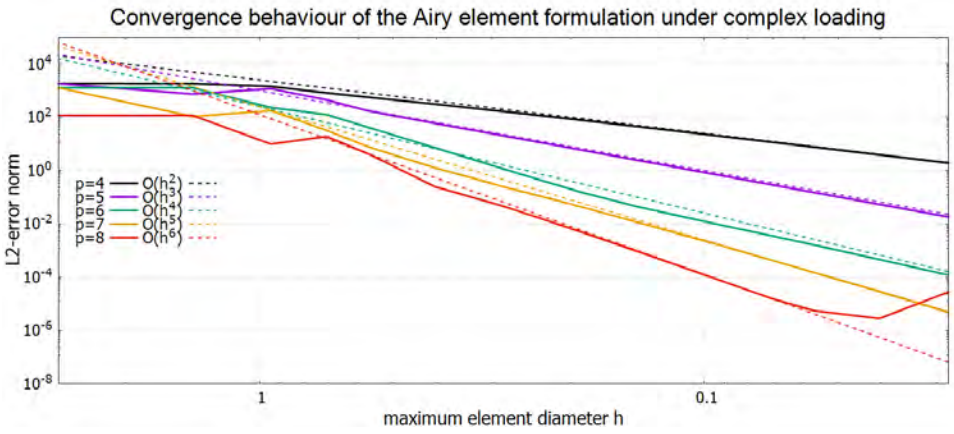

Figure 12: Convergence behaviour for the quadratic plate under complex load using orders $p = 4, .., 8$ for the discretization. The slopes can be seen to be around $p - 2$ for each curve.

Using the plot of the L_2-error norm in Fig. 12, the convergence behaviour of the proposed element formulation is assessed. To receive maximum C^{p-1} continuity, k-refinement is used. After some refinement steps a proper convergence behavior is obtained. All considered orders converge to the exact solution. The slope of the L_2 error norm of the stresses for a computation using basis functions of order p can be seen to be approximately equal to $p - 2$.

6 CONCLUSION

Within this work a one-degree of freedom formulation for two-dimensional linear elasticity problems has been obtained. It is based on the Airy equation and allows to compute stresses as direct solution of the underlying system of equations. Situations where only stress boundary conditions are relevant can be computed without defining suitable displacement boundary conditions. Thus, computations of that kind are strongly simplified. Possible applications could be the analysis on the micro level in an FE^2 formulation [10]. However, for that kind of applications it might be required to extend the formulation to handle non-rectangular meshes, which will be subject of future research. Within the described method the need for higher derivatives yields a more costly computation of the condition matrix, but the effort for the solution of the global system of equations will be significantly lower since just one degree of freedom per control point is required. Thus, the method can be competitive to a standard displacement-based

two-dimensional elasticity formulation. Future research will try to quantify this exactly. The presented formulation yields the exact solution in the first two simple examples as expected and shows proper convergence behavior in the third example with a very complex state of stress. Future work will focus on a mathematical proof of the convergence rates, on the imposition of displacement boundary conditions and the computation of arbitrarily shaped patches.

REFERENCES

[1] T. J. R. Hughes, J. A. Cottrell, and Y. Bazilevs, "Isogeometric analysis: Cad, finite elements, nurbs, exact geometry and mesh refinement," *Comput. Methods Appl. Mech. Engrg.*, vol. 194, pp. 4135–4195, 2005.

[2] L. Piegl and W. Tiller, *The NURBS book*, 2nd ed., ser. Monographs in visual communications. Berlin: Springer, 1997.

[3] J. A. Cottrell, T. J. R. Hughes, and Y. Bazilevs, *Isogeometric analysis: Toward integration of CAD and FEA*. Chichester: Wiley, 2009.

[4] T. J. R. Hughes, A. Reali, and G. Sangalli, "Efficient quadrature for nurbs-based isogeometric analysis," *Comput. Methods Appl. Mech. Engrg.*, vol. 199, pp. 301–313, 2010.

[5] R. R. Hiemstra, F. Calabrò, D. Schillinger, and T. J. Hughes, "Optimal and reduced quadrature rules for tensor product and hierarchically refined splines in isogeometric analysis," *Comput. Methods Appl. Mech. Engrg.*, vol. 316, pp. 966–1004, 2017.

[6] K. A. Johannessen, "Optimal quadrature for univariate and tensor product splines," *Comput. Methods Appl. Mech. Engrg.*, vol. 316, pp. 84–99, 2017.

[7] W. Dornisch and Y. Sikang, "Effiziente integrationsmethoden für isogeometrische schalenelemente," in *Berichte der Fachtagung Baustatik – Baupraxis 14*, M. Bischoff, M. von Scheven, and B. Oesterle, Eds. Stuttgart: Institut für Baustatik und Baudynamik, Universität Stuttgart, 2020, pp. 415–422.

[8] M. H. Gfrerer and M. Schanz, "Code verification examples based on the method of manufactured solutions for kirchhoff–love and reissner–mindlin shell analysis," *Eng. Comput.*, vol. 34, pp. 775–785, 2018.

[9] M. H. Sadd, *Elasticity: Theory, applications, and numerics*, 3rd ed. Amsterdam and Boston: Elsevier/Academic Press, 2014. [Online]. Available: http://www.sciencedirect.com/science/book/9780124081369

[10] S. Klarmann, F. Gruttmann, and S. Klinkel, "Homogenization assumptions for coupled multiscale analysis of structural elements: beam kinematics," *Comput. Mech.*, vol. 65, pp. 635–661, 2020.